Analysis of Wire-Cut Electro Discharge Machining of Polymer Composite Materials

Prayag Prajapati[1*], Naga Sai Prasad[2]

[1*]Assistant Professor, Department of Mechanical Engineering, Nalanda Institute of Technology, Bhubaneswar, Odisha, India

[2] Associate Professor, Department of Mechanical Engineering, Nalanda Institute of Technology, Bhubaneswar, Odisha, India

*Corresponding author e-mail: prayagprajapati@thenalanda.com

Abstract: In this study, wire-cut electro-discharge machining (WIRE-EDM) of polymer composite material is analysed (PCM). Using titanium plates (layers) that are 1 mm thick and sandwiched between the PCM improves the conductivity of the workpiece. Variable voltage (50-100 V), pulse duration (5-15 s), and pause time (10-50 s) are chosen as the input process parameters, and the cut-width (kerf) is recognised as an output parameter. Following the central composition design (CCD) design grid, experimentation was conducted. To explore the impact of process parameters on the cut-width of the PCM pieces and create the theoretical model, analysis of variance was used. The outcomes showed that voltage and pulse duration had a substantial impact on PCM's cut-width precision. Also, the theoretical model of machining is created and shows the effectiveness within the permitted range. The model is a great approach to accurately estimate the correction factors to machine complex-shaped PCM parts, it is concluded in the end.

Keywords: wire electro-discharge machining; polymer composite materials; processing precision; interelectrode gap

---

1. Introduction

In recent times, replacing metallic machine parts with composite materials has been considered a viable solution to a number of problems, such as excessive metal costs, rusting, and component weight. Composite materials with physical and mechanical qualities that are comparable to or even better than those of metals are highly encouraged in the current machining industry [1-3]. Polymer composite materials (PCMs) are acknowledged as a class of materials that are challenging to machine [4]. The creation of lightweight PCMs is essential for many vital industrial applications as well as aviation. These materials are cost-effective and lower the load of CO_2 emissions [1]. High elastic strength and operational stability are produced by the strong and heat-resistant binders employed in PCM. The ductile phase in the PCM, in contrast, is the matrix phase, which transfers the external load stress to the filler phase. The strength, stiffness, and deformability of a PCM are all mechanical qualities that depend on the filler/reinforcement employed in it. Carbon or ceramic fibres could be utilised as filler. These fibres have strong mechanical and physical characteristics. Through weaving, these fibres are transformed into cloths [5-7]. Figure 1a depicts a typical PCM, and the fibres' weaving pattern determines the reinforcement phase and potential flaws in traditional machining.
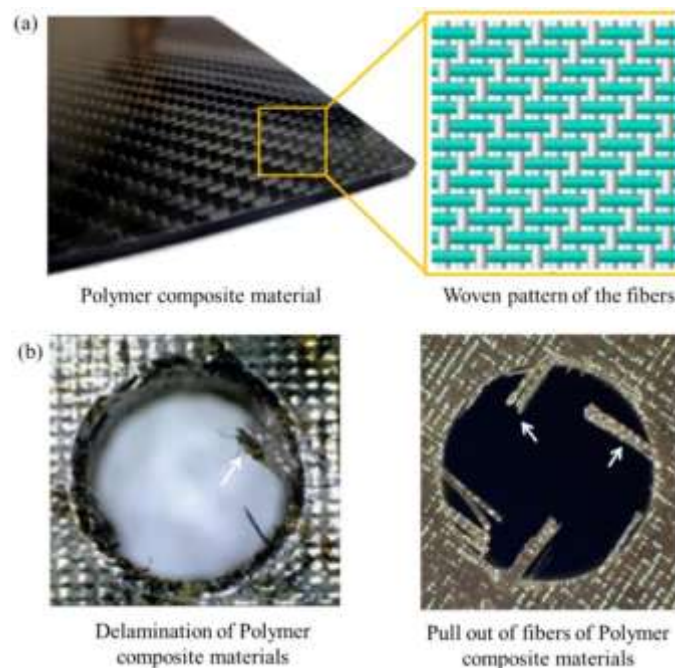
Figure 1. (**a**) Polymer composite materials and woven patterns of fibers of the reinforcement phase; and (**b**) delamination and pull out of fibers during the drilling of polymer composite materials.

PCMs possess many limitations during their machining due to mismatch of properties in the filler and matrix phases [8,9]. PCMs tend to delaminate during machining due to layering, structural heterogeneity, high hardness of the filler material, and low plasticity of the binder. The machining of PCMs also results in high cutting forces and vibrations, which causes pullout of fibers and other detrimental effects at the machined zone. Delamination and pull out of fibers can be observed in Figure 1b, which diminishes the quality of the fabricated feature. Moreover, during PCM machining, a high tool wear rate causes a decrease in productivity and enhances manufacturing costs. To avoid such problems, various non-conventional machining methods have been developed for processing these materials (Figure 2). Despite having many advantages over conventional machining methods, non-conventional processes such as electrochemical and chemical processing are hazardous to the environment [10,11]. On the other hand, techniques such as laser treatment [12–15], plasma treatment [16,17], electron beam treatment [18,19], ultrasonic treatment [20–22], and water jet treatment [23–27] are considered advantageous only where accuracy is not the primary concern. Moreover, these machining methods have disadvantages such as thermal destruction of the matrix phase and lack of accuracy, limiting their application for machining small-sized components.
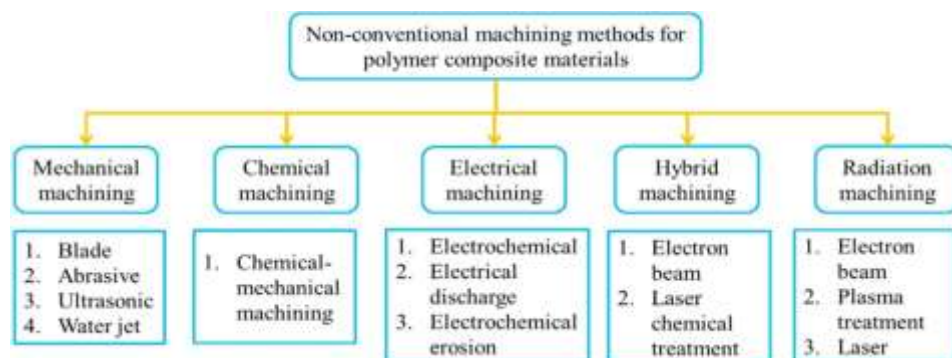

Figure 2. Non-conventional machining methods of polymer composite materials.

Among the various non-conventional machining techniques, Wire-cut Electrical Discharge machining (WIRE-EDM) has been proven to be a potential candidate to prepare small components with high accuracy [28–30]. In this process, thermal-electrical energy is involved in transforming the electrical energy to heat energy sufficient to melt the target zone, and an accurate curved profile can be obtained on metallic as well as polymer composite materials. A schematic diagram of the WIRE-EDM process is shown in Figure 3. In this process, the wire electrode moves vertically (mostly) over sapphire or diamond guides, which are controlled by Computer Numerical Control (CNC) program. A steady stream of deionized water or other fluid is used as a dielectric medium, flushes out debris, and cools the workpiece and the wire electrode. The dielectric fluid gets ionized, thereby producing a spark between the wire electrode tool (ET) and the workpiece electrode (WE) (Figure 3). The ionization of dielectric fluid depends on many factors of WIRE-EDM, such as properties of the working fluid, degree of contamination of the working fluid with erosion, the material of the electrodes, and dielectric flow pressure. The amount of thermal energy generated within the electrodes affects the amount of material removed from the surfaces of the ET and WE differently. This unevenness in material removal depends on the thermophysical properties of the ET and WE, and the process parameters of WIRE-EDM [29–31]. By varying these factors, electrode erosion can be precisely controlled. The spark energy within the electrodes depends on the voltage, the pulse formation time, the state of the working fluid, and the size of the interelectrode gap. Thus, the accuracy of the WIRE-EDM of PCMs is influenced by the size of the inter-electrode gap. The error of the inter-electrode gap depends on the inhomogeneity in the structures/properties of ET and the WE, and also the properties of the working fluid. The WIRE-EDM of PCMs results in the formation of dimples/craters of different sizes on the surface of the workpiece. These randomly formed dimples/craters are a factor that complicates the prediction of the inter-electrode gap [31].
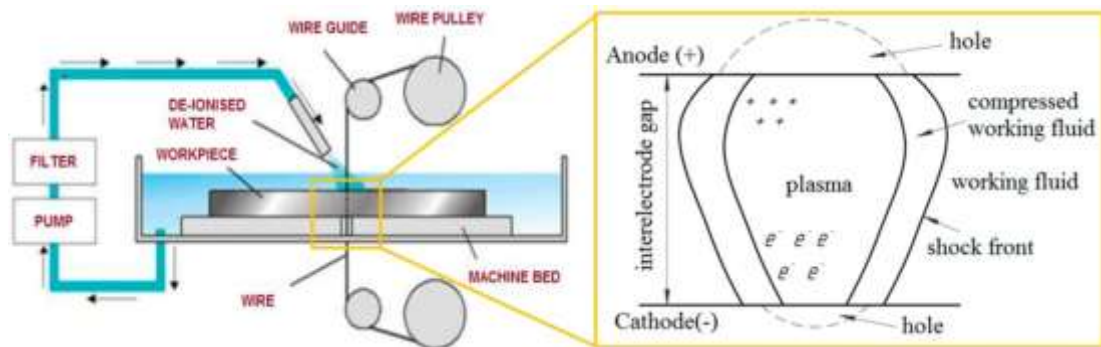

Figure 3. Schematic diagram and working principle of the wire-cut electro-discharge machining (WIRE-EDM) process [31].

The application of WIRE-EDM on PCMs has been investigated by various researchers [8,9]. However, it is a known fact that the conductivity of PCMs is limited. Thus, during the WIRE-EDM process, the resin of the PCM was destroyed at the edges of the holes. This was due to high temperatures and ineffective cooling at the machining zone.

Abdallah et al. [32] used WIRE-EDM to study the effects of gap voltage, current, pulse-on time, and pulse-off time on the material removal rate (MRR), top and bottom cut-width (kerf), and workpiece edge damage in unidirectional carbon fiber reinforced polymer (CFRP) composites. Current and pulse-off time were found to be statistically important parameters in terms of MRR, with current being the only factor affecting cut-width on the top surface. Recently, Dutta et al. [33] investigated a modified version of WIRE-EDM for CFRP composite cutting by using H13 steel plates as sandwich, assisting the electrodes to trigger the electrical spark during CFRP composite WIRE-EDM. Using metal plates (H13 steel) as assisting electrodes, problems such as incomplete cuts and deviations in the machining direction during CFRP WIRE-EDM were controlled. The results showed that

increasing the current (from 2A to 12A) reduced the cutting time (by 60.95%) while keeping all other parameters constant.

Likewise, in similar studies [34–48] related to the WIRE-EDM of PCMs, it was observed that the quality and accuracy of holes in a low-conductive material can be regulated by applying a conductive layer above the non-conductive PCM. Also, the development of theoretical models of the WIRE-EDM of PCMs provides a guide to obtain the accuracy required in the process [37].

A schematic of WIRE-EDM process is represented in Figure 4. Herein, the size of the ET (2R), and the value of interelectrode gap(overcut)S are taken into account for accurate machining of the product. The correction in machining can be done in reference to the center of the ET(wire)in a CNC controller.
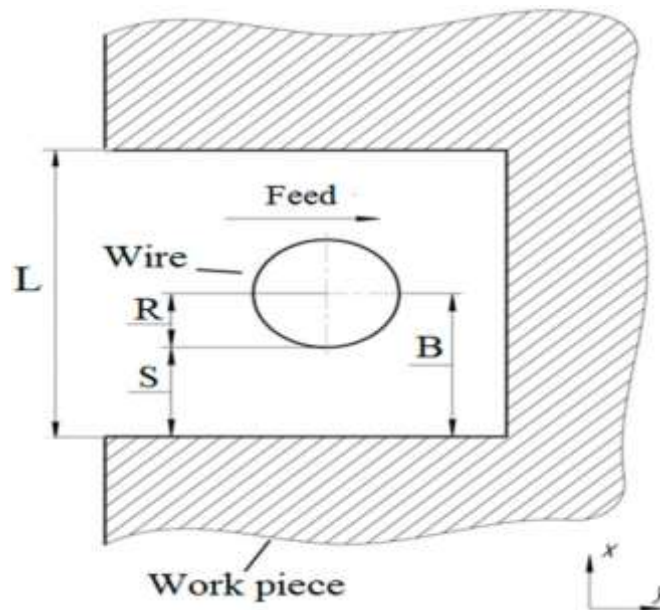

Figure 4. WIRE-EDM processing in the XY plane: R—radius of the electrode tool (ET); S—interelectrode gap;(B)—reference for correction; L—cut-width (Kerf).

The material removal rate from the workpiece during a single pulse is estimated by the following equation [49–51]:

$$MRR = \frac{m}{t_{on}} \tag{1}$$

where t_{on} is the duration of a single pulse (μs), and m is the weight lost during the EDM process (kg). Data in the literature [31,51] indicate that MRR depends on the value of the interelectrode gap S (m), the feed rate V (m/s), the physical and mechanical properties of the processed material, and the workpiece thickness h (m). MRR is calculated using Equation (2):

$$MRR = 2(R + S)hV\rho \tag{2}$$

where R is the radius of the ET (m), S is the interelectrode gap (m); ρ is the density of the processed material (kg/m^3), h is the thickness of workpiece (m), and V is the feed rate.

The spark energy, W (J), is released in the interelectrode gap and is distributed between the ET and the workpiece. The material is removed from the workpiece by the mean of the spark energy [31]. The pulse energy is calculated as:

$$W = \int_{0}^{t_p} UIdt_{on} \tag{3}$$

where U is the voltage, (V); I is the current strength, (A); t_{on} is the pulse duration, (µs); and tp is the pulse width (µs). A correction factor is introduced in Equation (3) to improve the accuracy of the calculations.

$$W = (\eta_u)UIt_{on} \qquad (4)$$

The coefficient for a fraction of the energy (η_u) utilized in the machining process is represented in Equation (5) [31,50]:

$$\eta_u = (1 - K_1)(1 - K_2) \qquad (5)$$

where K_1 is the amount of energy lost during the heating and evaporation of the dielectric fluid; K_2 is amount of energy lost in the ET. The amount of heat Q (J) transferred to the WE for heating and melting is determined by the formula:

$$Q = m(C_1\Delta T_1 + \lambda + C_2\Delta T_2 + r) \qquad (6)$$

where m is the mass of the workpiece (kg); C_1 is the specific heat capacity of the material in the solid state (J/kg K) C_2 is the specific heat capacity of the material in the liquid state (J/kg K); ΔT is the temperature difference between the initial and final heating points (K); λ is the specific heat of fusion of the material (J/kg); and r is the specific heat of vaporization (J/kg).

Taking into the account the equal coefficients of energy loss in Equation (4) and Equation (6) (i.e., W and Q) and $Z = C_1\Delta T_1 + \lambda + C_2\Delta T_2 + r$. Equation (1) is represented as:

$$MRR = \frac{Q\eta_uUI}{ZW} = \frac{\eta_uUI}{Z} \qquad (7)$$

thus equating expressions (2) and (7). The value of the interelectrode gap S is calculated as:

$$S = \frac{\eta_uUI}{2ZhV\rho} - R \qquad (8)$$

The value of B (as shown in Figure 4) can be calculated, and thus the cut width (L) is obtained. This theoretical model can be used to estimate the process parameter affecting the cut width (L), and can thus suggest the amount of correction required for accurate machining.

The PCM is made up of both electrically conductive carbon fiber and non-conductive epoxy resin. As a result, machining such composites with prominent machining techniques i.e., WIRE-EDM or EDM is a difficult job. In the literature, research on the WIRE-EDM of PCM is limited to where the effect of WIRE-EDM on PCM is explored for higher machining rate, electrode wear, and performance in the linear cut.

In this work, the authors investigated the performance of WIRE-EDM on a patent carbon fiber-reinforced PCM possibly adopted in the aviation industry. The voltage, pulse duration, and pause time were selected as process parameters. These parameters were statistically evaluated, and the level of the significance of factors affecting the cut width was determined using analysis of variance. Finally, the experimental values obtained for cut width were modeled mathematically in terms of significant factors using response surface methodology.

Purpose of Study
- To assess the influence of key process parameters on the cut width (kerf) and surface quality of PCM sandwiched in Titanium alloy.
- To develop a regression model using response surface methodology, which is further examined with the experimental results for non-linear machining cut-width on the selected PCM.
- To determine the trajectory of ET to machine PCM in the form of a complex shaped part, such as a gear.

2. Material and Methods

Material

In this study, a polymer composite material (VKU-39, pl. refer https://viam.ru, 11 May 2021) used in the aviation industry was chosen. The workpiece is a laminated fibrous polymer composite made of carbon fiber twill as reinforcement/filler, with epoxy as a binder material. The property of the selected PCM is as shown in Table 1.

Table 1. Properties of polymer composite material (PCM).

Property	Average Value
Filler material	Carbon fabrics twill (Porcher-3692)
Heat resistance $^{\circ}$C	170°
Monolayer thickness, mm	0.2
Tensile strength, MPA	945
Tensile modulus, GPA	69
Compressive strength, MPA	610
Compression modulus, GPA	54
Density of carbon fiber reinforced polymer (CFRP), kg/m^3	1550
Weaving type	Twill, at an angle of 90°
Electrical conductivity, S/m	10^{-7}

A PCM plate of thickness 2 mm was used for the WIRE-EDM experiments. To improve the conductivity of the PCM, a conductive layer of titanium (1 mm) was applied on both sides (Figure 5). The study was carried out on a wire-cut EDM machine, "Electronica EcoCut." The electrode tool (ET) used was a brass wire with a diameter of 0.25 mm. Distilled water was used as a dielectric medium, and was sprayed on the ET (Figure 5) instead of immersing the PCMs in a water bath, as PCM immersion in a water bath causes defects such as swelling and filling of water.
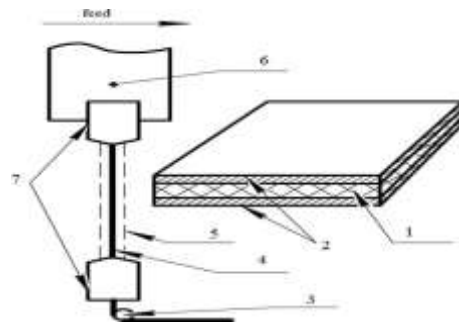

Figure 5. Schematic of the WIRE-EDM of polymer composite material (PCM) with conductive layers used in the present study (1: PCM, 2: conductive Ti-layers, 3: tension roller, 4: ET wire, 5: flushing, 6: gearbox, 7: upper and lower diamond wire guides).

Method

The process parameters selected were U—voltage, V; Ton—pulse duration, μs; and Toff—the pause time in pulse duration. The experimental runs were carried out by employing the orthogonal central composition design (CCD) matrix, where α denotes the distance between the star point and central point i.e., value of α = 1.215. The design matrix in the study was obtained with the assistance of Design-Expert software. Orthogonality in the design assisted in estimating the independent regression coefficients [49,52]. The process parameters are presented in Table 2. The output parameter was the value of the EDM cut width (L). The cut width was the wire diameter of the ET and the size of the side clearance (overcut).

Table 2. Process parameters of wire-electrical discharge machining (EDM).

Factors, Units	Units	Lower Level(−1)	Upper Level(+1)	Average Level	Lower "Star" Point	Top "Star" Point
U	V	50	100	75	40	110
Ton	μs	5	15	10	2	20
Toff	μs	10	50	30	5	60

The experiment design matrix and response (cut width) is presented in Table 3. Each experimental run was replicated thrice for more accuracy. A pictorial view of the machining process is shown in Figure 6.

Table 3. Experimental central composition design (CCD) matrix with the responses the experiment obtained.

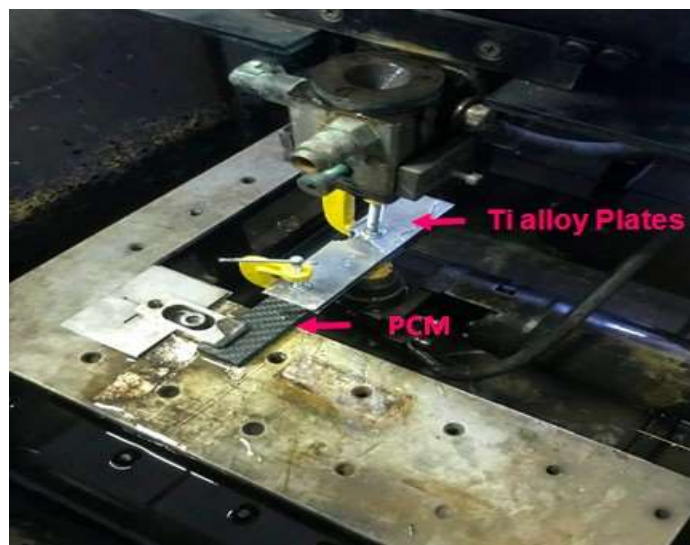| Exp. No.	Process Parameters			Response
	Voltage U (V)	Pulse Duration Ton (μs)	Pause Time Toff (μs)	Cut-Width L (μm)
1	100	15	50	337
2	50	15	10	286
3	100	5	50	280
4	75	10	60	323
5	75	10	5	327
6	50	5	10	275
7	50	5	50	284
8	75	20	30	355
9	100	15	10	342
10	50	15	50	276
11	75	2	30	273
12	110	10	30	315
13	75	10	30	294
14	100	5	10	255
15	40	10	30	283

Figure 6. Pictorial view of PCM machining setup.

3. Results and Discussion

Analysis of variance (ANOVA) is a commonly used statistical technique to test the significance of a model and the contribution of each process parameter on the experimental

response. The mathematical model was predicted using Design Expert software and is summarized in Table 4.

From Table 4, it is observed that the value of adjusted R-square and predicted R-square values were higher for the 2-way interaction model. Thus, this model is suggested for further analysis.

Statistical analysis of the experimental data (Table 5) revealed the significance of the process parameters, namely voltage, pulse duration, and pause time, on the measured response i.e., cut width. The results are summarized in Table 5, with a 95% confidence level.

Table 4. Mathematical model analysis.

Model	p-Value	Adjusted R^2	Predicted R^2	
Linear	0.0127	0.5061	0.2412	-
2-way interaction	0.0663	**0.7100**	**0.3711**	Suggested Model
Quadratic	0.4820	0.7049	−0.0121	-

Table 5. Analysis of variance (ANOVA) of process parameters for 2-way interaction model.

ANOVA for Response Surface						
Source	**Sum of Squares**	**df**	**Mean Square**	**F-Value**	**p-Value**	
Model	10,655.21	6	1775.87	6.71	0.0085	Significant
U-Voltage	1593.02	1	1593.02	6.02	0.0397	-
Ton	6189.06	1	6189.06	23.40	0.0013	-
Toff	33.21	1	33.21	0.1256	0.7322	-
U × Ton	2485.13	1	2485.13	9.40	0.0155	-
U × Toff	55.13	1	55.13	0.2084	0.6602	-
Ton × Ton	300.12	1	300.12	1.13	0.3179	-
Residual	2116.12	8	264.52	-	-	-
Total	12,771.33	14	1775.87	-	-	-

The 2-way interaction model F-value of 6.71 implies that the model is significant, and only 0.85% chance of noise exists in this model. From Table 5, the p-value less than 0.05 indicated that the model terms of voltage, Ton, and their interaction (i.e., U× T-on) were significant, whereas Toff, U× Toff and Ton×Ton were insignificant. Eliminating insignificant terms results in the improvement in the model, as presented in Table 6.

Table 6. ANOVA for the reduced 2-way interaction model.

ANOVA for Response Surface						
Source	**Sum of Squares**	**df**	**Mean Square**	**F-Value**	**p-Value**	
Model	10,266.75	3	3422.25	15.03	0.0003	Significant
U-Voltage	1593.02	1	1593.02	7.00	0.0228	-
Ton	6188.60	1	6188.60	27.18	0.0003	-
U × Ton	2485.13	1	2485.13	10.91	0.0070	-
Residual	2504.58	11	227.69	-	-	-
Total	12,771.33	14	3422.25	-	-	-

The model regression statistics for the selected model demonstrated a high R^2 value (i.e., 0.80), which is acceptable. The predicted R^2 of 0.6677 was in reasonable agreement with the adjusted R^2 of 0.7504; i.e., the difference was less than 0.2.

In order to check the adequacy of model, the predicted value and the actual experimental values were compared along a 45° line, as shown in Figure 7. This implies that the proposed model is adequate and there is no violation of the independent or constant variance assumptions.
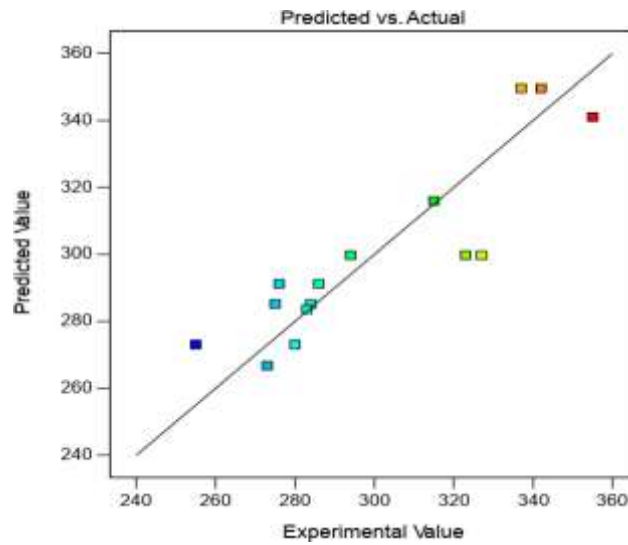
Figure 7. Comparison of model-predicted values versus actual experiment values for cut width.

The final equation obtained for the prediction of cut-width (L) is represented as Equation (9):

$$L = 329.6 - 0.9475 \times U - 6.45 \times Ton + 0.141 \times U \times Ton \qquad (9)$$

The regression equation analysis (9) shows the combination (interaction) of input process parameters (factors) affecting the value of the cut width.

Figures 8 and 9 presents the response surface describing the dependence of the cut width on the voltage and pulse duration.
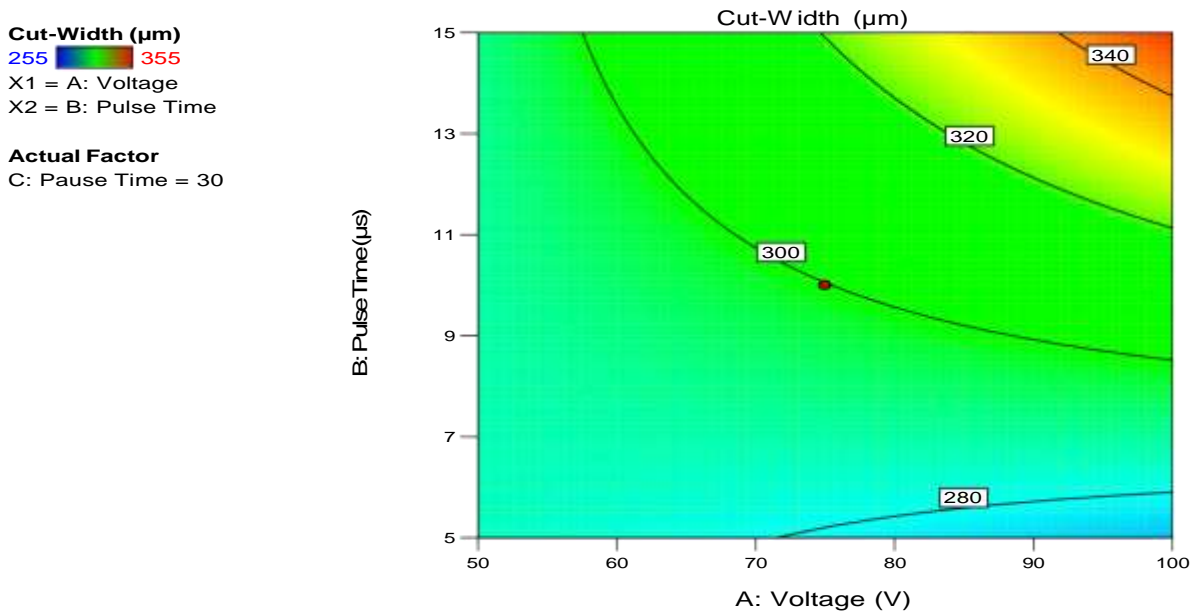
Figure 8. Contour plot for cut-width dependance on voltage and pulse duration for pause time Toff = 30 μs.

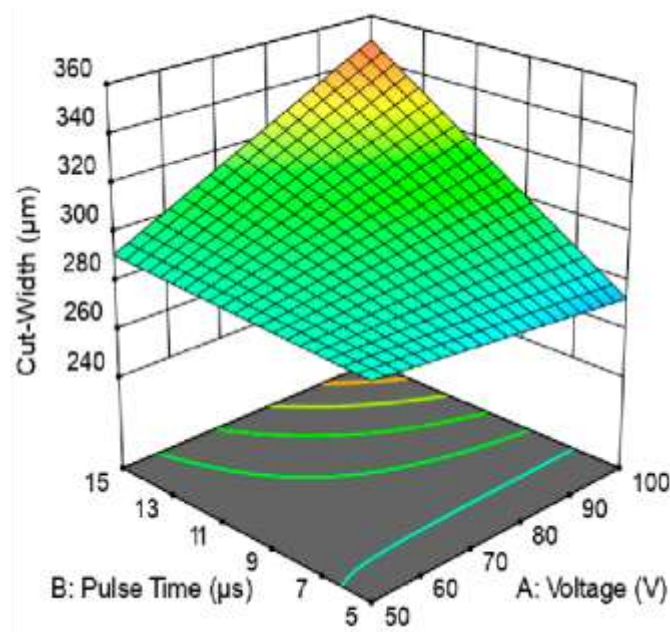**Figure 9.** Response surface 3D-plot for cut-width dependence on voltage and pulse duration for pause time Toff = 30μs.

Examination of the Predicted Model forWIRE-EDM onComplex-Shaped PCM Parts

It is depicted from the plots (Figures 8 and 9) that cut width is directly proportional to the voltage and pulse duration. Thus, for machining complex PCM parts, a high value for WIRE-EDM i.e., U = 100 V, Ton = 15 μs, Toff = 30 μs was selected. The obtained cut width path is presented in Figure 10. The cut width (Figure 10) was measured at various WIRE-EDM zones, i.e., at the entrance to the PCM, at the corner, and the end of processing. The average value of the cut width was calculated as L = 330 μm.
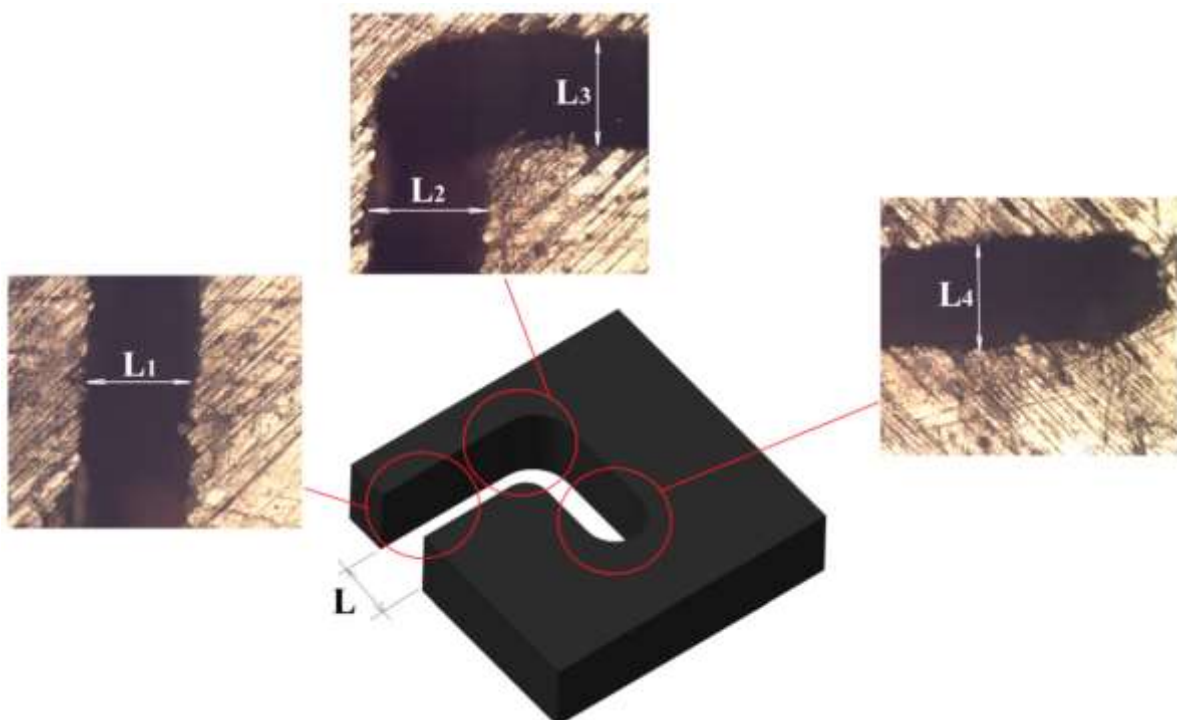

Figure 10. Values of the cut width for PCM wire-cut electro-discharge machining (WIRE-EDM) at U = 100 V, Ton = 15 μs, Toff = 30 μs: L_1 = 325 μm, L_2 = 345 μm, L_3 = 325 μm, L_4 = 330 μm.

Figure 11a,b reveals the surface the cutting edge achieved after applying the conductive Ti-alloy layer (plates) to the surface of PCM. It is found that this method of machining results in attaining a defect-free smooth surface on both sides of the processed PCM sheet at the entrance, at the corner, and at the end.
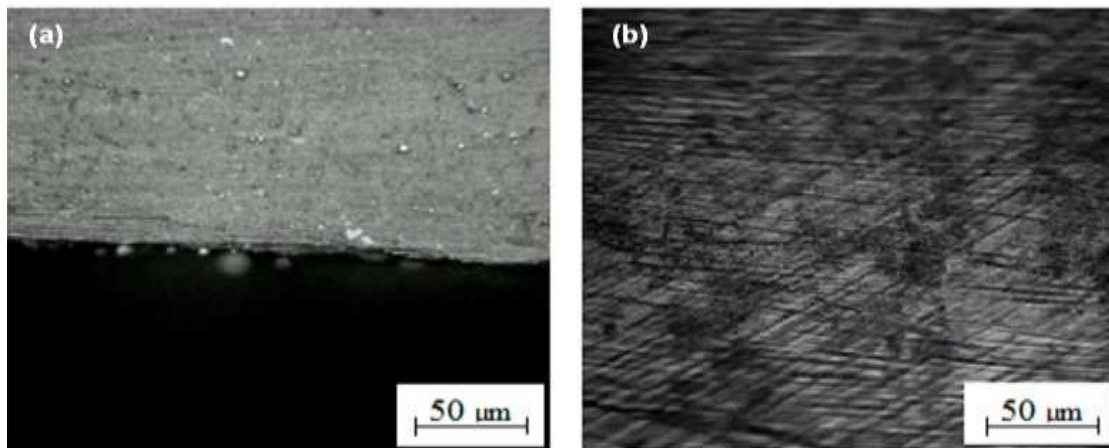

Figure 11. Machined PCM surfaces after application of a conductive Ti-layer on the surface of PCM; (**a**)—sheet surface at the processing zone (at the edge), (**b**)—along the cross-section of sheet width.

Thus, the Ti layer sandwich method for PCM enhanced the quality of the machined surface. Additionally, it has the potential to obtain a smooth, defect-free surface within the processed slot without causing any damage to the fibers/binder of the PCM material.

The percentage error between the values of the cut-width was calculated using Equation (10). The expected value from Equation (9) was calculated as 349.6 µm, and the experimental value (actual value) measured was 330 µm (Figure 10). Thus, the percentage error obtained is calculated as 5.906%, which is acceptable and shows the competency of the model.

$$\% \; error \; = \; \frac{|Expected \; value \; - \; Actual \; value|}{Expected \; value} \tag{10}$$

The regression Equation (9) was further examined to accurately machine a gear-shaped PCM part. An "Electronica EcoCut" CNC WIRE-EDM machine was programmed. The program was used to machine a PCM workpiece into the gear shape. The machining parameters were carried out at Ton = 15µs, Toff = 30 µs, and U = 100 V. Based on this regression model (Equation (9)), the trajectory correction value was calculated as B = 0.165 mm. When machining the PCM, the offset was added into the control program using the command "G41 B" = 0.165. In Figure 12, the trajectory of the ET and the finished product "gear" are presented.
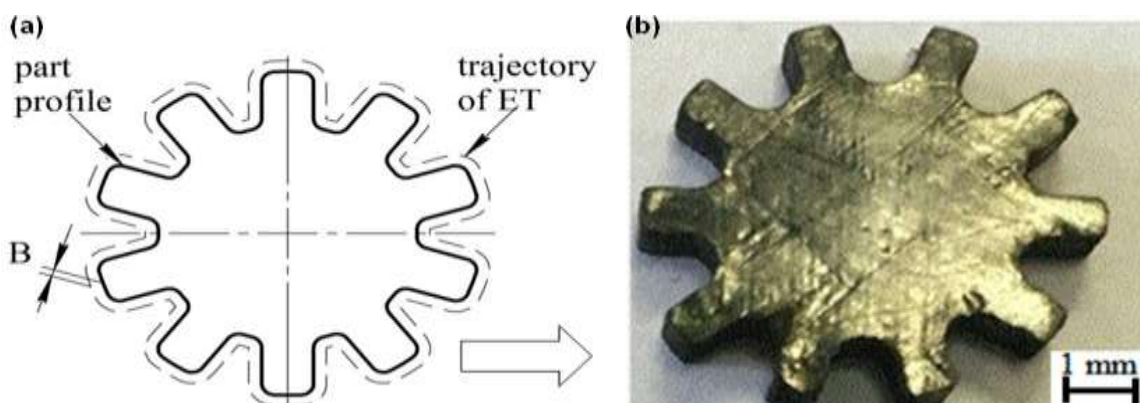

Figure 12. (**a**) Trajectory of the ET, and (**b**) finished product.

4. Conclusions

The experimental work demonstrates the relationship between WIRE-EDM processing parameters such as voltage, pulse-on time, and pulse-off time and the cut width. These outcomes can be accelerated to increase the ET's size and guarantee accuracy in the WIRE-EDM of PCM (VKU-39) workpieces. It is determined that the key variables influencing the process parameters for milling the PCM workpiece are voltage, pulse duration, and their interaction. A 2-way interaction model is also created to estimate the cut-width, and it exhibits great agreement with the results of the experiments. In order to accurately make a complex-shaped PCM product, the cut-width correction factor for the trajectory of ET was predicted using the created model in a WIRE-EDM CNC machine. The forecasting of WIRE-EDM accuracy is thus said to be successfully facilitated by the proposed model.

References

1. Sarde, B.; Patil, Y.D. Recent Research Status on Polymer Composite Used in Concrete—An Overview. *Mater. Today Proc.* **2019**, *18*, 3780–3790. [CrossRef]
2. Yahaya, R.; Sapuan, S.; Jawaid, M.; Leman, Z.; Zainudin, E. Mechanical performance of woven kenaf-Kevlar hybrid composites. *J. Reinf. Plast. Compos.* **2014**, *33*, 2242–2254. [CrossRef]
3. Hsissou, R.; Benhiba, F.; Echihi, S.; Benkhaya, S.; Hilali, M.; Berisha, A.; Briche, S.; Zarrouk, A.; Nouneh, K.; Elharfi, A. New epoxy composite polymers as a potential anticorrosive coatings for carbon steel in 3.5% NaCl solution: Experimental and computational approaches. *Chem. Data Collect.* **2021**, *31*, 100619. [CrossRef]
4. Valino, A.D.; Dizon, J.R.C.; Espera, A.H.; Chen, Q.; Messman, J.; Advincula, R.C. Advances in 3D printing of thermoplastic polymer composites and nanocomposites. *Prog. Polym. Sci.* **2019**, *98*, 101162. [CrossRef]
5. Hsissou, R.; Bekhta, A.; Dagdag, O.; El Bachiri, A.; Rafik, M.; Elharfi, A. Rheological properties of composite polymers and hybrid nanocomposites. *Heliyon* **2020**, *6*, e04187. [CrossRef]
6. Mehra, N.; Mu, L.; Ji, T.; Yang, X.; Kong, J.; Gu, J.; Zhu, J. Thermal transport in polymeric materials and across composite interfaces. *Appl. Mater. Today* **2018**, *12*, 92–130. [CrossRef]
7. Thomason, J. A review of the analysis and characterisation of polymeric glass fibre sizings. *Polym. Test.* **2020**, *85*, 106421. [CrossRef]
8. Shlykov, E.S.; Ablyaz, T.R.; Oglezneva, S.A. Electrical Discharge Machining of Polymer Composites. *Russ. Eng. Res.* **2020**, *40*, 878–879. [CrossRef]
9. Ablyaz, T.R.; Muratov, K.R.; Shlykov, E.S.; Shipunov, G.S.; Shakirzyanov, T.V. Electric-Discharge Machining of Polymer Composites. *Russ. Eng. Res.* **2019**, *39*, 898–900. [CrossRef]
10. Yao, Y.; Wang, B.; Wang, J.; Jin, H.; Zhang, Y.; Dong, S. Chemical machining of Zerodur material with atmospheric pressure plasma jet. *CIRP Ann.* **2010**, *59*, 337–340. [CrossRef]
11. Shimpi, J.R.; Sidhaye, D.S.; Prasad, B.L. Digestive Ripening: A Fine Chemical Machining Process on the Nanoscale. *Langmuir* **2017**, *33*, 9491–9507. [CrossRef] [PubMed]
12. Romoli, L.; Tantussi, G.; Dini, G. Experimental approach to the laser machining of PMMA substrates for the fabrication of microfluidic devices. *Opt. Lasers Eng.* **2011**, *49*, 419–427. [CrossRef]
13. Li, Z.; Zheng, H.; Lim, G.; Chu, P.; Li, L. Study on UV laser machining quality of carbon fibre reinforced composites. *Compos. Part A Appl. Sci. Manuf.* **2010**, *41*, 1403–1408. [CrossRef]
14. Samant, A.N.; Dahotre, N.B. Laser machining of structural ceramics—A review. *J. Eur. Ceram. Soc.* **2009**, *29*, 969–993. [CrossRef]
15. Pham, D.T.; Dimov, S.S.; Ji, C.; Petkov, P.V.; Dobrev, T. Laser milling as a 'rapid' micromanufacturing process. *Proc. Inst. Mech. Eng. Part B J. Eng. Manuf.* **2004**, *218*, 1–7. [CrossRef]

16. Shi, B.; Dai, Y.; Xie, X.; Li, S.; Zhou, L. Arc-Enhanced Plasma Machining Technology for High Efficiency Machining of Silicon Carbide. *Plasma Chem. Plasma Process.* **2016**, *36*, 891–900. [CrossRef]

17. Malhotra, R.; Saxena, I.; Ehmann, K.F.; Cao, J. Laser-induced plasma micro-machining (LIPMM) for enhanced productivity and flexibility in laser-based micro-machining processes. *CIRP Ann.* **2013**, *62*, 211–214. [CrossRef]

18. Spinney, P.S.; Howitt, D.G.; Smith, R.L.; Collins, S.D. Nanopore formation by low-energy focused electron beam machining. *Nanotechnology* **2010**, *21*, 375301. [CrossRef]

19. Parthasarathy, J.; Starly, B.; Raman, S.; Christensen, A. Mechanical evaluation of porous titanium (Ti6Al4V) structures with electron beam melting (EBM). *J. Mech. Behav. Biomed. Mater.* **2010**, *3*, 249–259. [CrossRef]

20. Koike, M.; Martinez, K.; Guo, L.; Chahine, G.; Kovacevic, R.; Okabe, T. Evaluation of titanium alloy fabricated using electron beam melting system for dental applications. *J. Mater. Process. Technol.* **2011**, *211*, 1400–1408. [CrossRef]

21. Rajurkar, K.; Sundaram, M.; Malshe, A. Review of Electrochemical and Electrodischarge Machining. *Procedia CIRP* **2013**, *6*, 13–26. [CrossRef]

22. Tiwari, A.; Mandal, A.; Kumar, K. Multi-objective Optimization of Electro-chemical Machining by Non-dominated Sorting Genetic Algorithm. *Mater. Today Proc.* **2015**, *2*, 2569–2575. [CrossRef]

23. Alberdi, A.; Rivero, A.; de Lacalle, L.N.L.; Etxeberria, I.; Suárez, A. Effect of process parameter on the kerf geometry in abrasive water jet milling. *Int. J. Adv. Manuf. Technol.* **2010**, *51*, 467–480. [CrossRef]

24. Ting, H.; Abou-El-Hossein, K.; Chua, H. Review of micromachining of ceramics by etching. *Trans. Nonferrous Met. Soc. China* **2009**, *19*, S1–S16. [CrossRef]

25. Matsumura, T.; Muramatsu, T.; Fueki, S. Abrasive water jet machining of glass with stagnation effect. *CIRP Ann.* **2011**, *60*, 355–358. [CrossRef]

26. Gupta, V.; Pandey, P.; Garg, M.P.; Khanna, R.; Batra, N. Minimization of Kerf Taper Angle and Kerf Width Using Taguchi's Method in Abrasive Water Jet Machining of Marble. *Procedia Mater. Sci.* **2014**, *6*, 140–149. [CrossRef]

27. Deris, A.M.; Zain, A.M.; Sallehuddin, R. A note of hybrid GR-SVM for prediction of surface roughness in abrasive water jet machining: A response. *Meccanica* **2017**, *52*, 1993–1994. [CrossRef]

28. Panner Selvam, M.; Ranjith Kumar, P. Optimization Kerf Width and Surface Roughness in Wirecut Electrical Discharge Machining Using Brass Wire. *Mech. Mech. Eng.* **2017**, *21*, 37–55.

29. Maher, I.; Ling, L.H.; Sarhan, A.A.D.; Hamdi, M. Improve wire EDM performance at different machining parameters—ANFIS modeling. *IFAC-PapersOnLine* **2015**, *48*, 105–110. [CrossRef]

30. Wu, C.; Cao, S.; Zhao, Y.J.; Qi, H.; Liu, X.; Liu, G.; Guo, J.; Li, H.N. Preheating assisted wire EDM of semi-conductive CFRPs: Principle and anisotropy. *J. Mater. Process. Technol.* **2021**, *288*, 116915. [CrossRef]

31. Abbas, N.M.; Solomon, D.G.; Bahari, F. A review on current research trends in electrical discharge machining (EDM). *Int. J. Mach. Tools Manuf.* **2007**, *47*, 1214–1228. [CrossRef]

32. Abdallah, R.; Soo, S.L.; Hood, R. A feasibility study on wire electrical discharge machining of carbon fibre reinforced plastic composites. *Procedia CIRP* **2018**, *77*, 195–198. [CrossRef]

33. Dutta, H.; Debnath, K.; Sarma, D.K. Investigation on cutting of thin carbon fiber-reinforced polymer composite plate using sandwich electrode-assisted wire electrical-discharge machining. *Proc. Inst. Mech. Eng. Part E J. Process. Mech. Eng.* **2021**. [CrossRef]

34. Fukuzawa, Y.; Katougi, H.; Mohri, N.; Furutani, K.; Tani, T. Machining properties of ceramics with an electric discharge machine. In Proceedings of the XII ISEM, Aachen, Germany, 11–13 May 1998; pp. 445–454.

35. Mohri, N.; Fukuzawa, Y.; Tani, T.; Saito, N.; Furutani, K. Assisting Electrode Method for Machining Insulating Ceramics. *CIRP Ann.* **1996**, *45*, 201–204. [CrossRef]

36. Mohri, N.; Fukusima, Y.; Fukuzawa, Y.; Tani, T.; Saito, N. Layer Generation Process on Work-piece in Electrical Discharge Machining. *CIRP Ann.* **2003**, *52*, 157–160. [CrossRef]

37. Lauwers, B.; Kruth, J.; Liu, W.; Eeraerts, W.; Schacht, B.; Bleys, P. Investigation of material removal mechanisms in EDM of composite ceramic materials. *J. Mater. Process. Technol.* **2004**, *149*, 347–352. [CrossRef]

38. Puertas, I.; Luis, C. A study on the electrical discharge machining of conductive ceramics. *J. Mater. Process. Technol.* **2004**, *153–154*, 1033–1038. [CrossRef]

39. Kucukturk, G.; Cogun, C. A New Method for Machining of Electrically Nonconductive Workpieces Using Electric Discharge Machining Technique. *Mach. Sci. Technol.* **2010**, *14*, 189–207. [CrossRef]

40. Hösel, T.; Müller, C.; Reinecke, H. Spark erosive structuring of electrically nonconductive zirconia with an assisting electrode. *CIRP J. Manuf. Sci. Technol.* **2011**, *4*, 357–361. [CrossRef]

41. Wüthrich, R.; Fascio, V. Machining of non-conducting materials using electrochemical discharge phenomenon—An overview. *Int. J. Mach. Tools Manuf.* **2005**, *45*, 1095–1108. [CrossRef]

42. Schubert, A.; Zeidler, H.; Wolf, N.; Hackert, M. Micro Electro Discharge Machining of Electrically Nonconductive Ceramics. In Proceedings of the 14th International Esaform Conference on Material Forming: ESAFORM 2011, Belfast, UK, 27–29 April 2011; AIP Publishing: College Park, MD, USA, 2011; pp. 1303–1308.

43. Saleh, M.; Anwar, S.; El-Tamimi, A.; Mohammed, M.K.; Ahmad, S. Milling Microchannels in Monel 400 Alloy by Wire EDM: An Experimental Analysis. *Micromachines* **2020**, *11*, 469. [CrossRef] [PubMed]

44. Kumar, V.; Kumar, V.; Jangra, K.K. An experimental analysis and optimization of machining rate and surface characteristics in WEDM of Monel-400 using RSM and desirability approach. *J. Ind. Eng. Int.* **2015**, *11*, 297–307. [CrossRef]
45. Manjaiah, M.; Narendranath, S.; Basavarajappa, S. Wire Electro Discharge Machining Performance of TiNiCu Shape Memory Alloy. *Silicon* **2016**, *8*, 467–475. [CrossRef]
46. Ahmed, N.; Mughal, M.P.; Shoaib, W.; Raza, S.F.; Alahmari, A.M. WEDM of Copper for the Fabrication of Large Surface-Area Micro-Channels: A Prerequisite for the High Heat-Transfer Rate. *Micromachines* **2020**, *11*, 173. [CrossRef] [PubMed]
47. Korlos, A.; Tzetzis, D.; Mansour, G.; Sargis, D.; David, C. The delamination effect of drilling and electro-discharge machining on the tensile strength of woven composites as studied by X-ray computed tomography. *Int. J. Mach. Mach. Mater. (IJMMM)* **2016**, *18*, 426–448. [CrossRef]
48. Wang, R.; Wang, J.; Yuan, W. Analysis and Optimization of a Microchannel Heat Sink with V-Ribs Using Nanofluids for Micro Solar Cells. *Micromachines* **2019**, *10*, 620. [CrossRef]
49. Yamada, H.; Mohri, N.; Furutani, K.; Saito, N.; Magara, T. Transient Response of Wire Vibration System in Wire Electrical Discharge Machining. *J. Jpn. Soc. Precis. Eng.* **1997**, *63*, 1548–1552. [CrossRef]
50. Enache, S.; Opran, C. Dynamic Stability of the Technological Machining System in EDM. *Ann. CIRP* **1993**, *42*, 209–214. [CrossRef]
51. Yan, M.-T.; Lai, Y.-P. Surface quality improvement of wire-EDM using a fine-finish power supply. *Int. J. Mach. Tools Manuf.* **2007**, *47*, 1686–1694. [CrossRef]
52. Schneider, A.; Hommel, G.; Blettner, M. Linear Regression Analysis: Part 14 of a Series on Evaluation of Scientific Publications. *Dtsch. Aerzteblatt Online* **2010**, *107*, 776–782. [CrossRef]